Accepted Manuscript

Hydrolytic degradation of D-mannitol-based polyurethanes

Lucía Romero-Azogil, Elena Benito, Antxon Martínez de Ilarduya, M.Gracia García-Martín, Juan A. Galbis

PII: S0141-3910(18)30156-3

DOI: 10.1016/j.polymdegradstab.2018.05.009

Reference: PDST 8543

To appear in: *Polymer Degradation and Stability*

Received Date: 15 March 2018

Revised Date: 23 April 2018

Accepted Date: 4 May 2018

Please cite this article as: Romero-Azogil Lucí, Benito E, de Ilarduya AntxonMartí, García-Martín MG, Galbis JA, Hydrolytic degradation of D-mannitol-based polyurethanes, *Polymer Degradation and Stability* (2018), doi: 10.1016/j.polymdegradstab.2018.05.009.

This is a PDF file of an unedited manuscript that has been accepted for publication. As a service to our customers we are providing this early version of the manuscript. The manuscript will undergo copyediting, typesetting, and review of the resulting proof before it is published in its final form. Please note that during the production process errors may be discovered which could affect the content, and all legal disclaimers that apply to the journal pertain.

ACCEPTED MANUSCRIPT

Hydrolytic degradation of D-mannitol-based polyurethanes

Lucía Romero-Azogil,[†] Elena Benito,[†] Antxon Martínez de Ilarduya,[‡] M. Gracia García-Martín[†]* and Juan A. Galbis[†]

[†]*Departamento de Química Orgánica y Farmacéutica, Facultad de Farmacia, Universidad de Sevilla, C/ Profesor García González 2, 41012-Sevilla, Spain*

[‡]*Departament d'Enginyeria Química, Universitat Politecnica de Catalunya, ETSEIB, Diagonal 647, 08028 Barcelona, Spain*

**Corresponding author: graciagm@us.es*

ABSTRACT

The capacity of redox D-mannitol-based polyurethanes to modulate the glutathione response under physiological conditions, as well as their effectiveness for sustained and site-specific drug release in the gastrointestinal tract (GIT), have been demonstrated in previous studies. Based on those promising results, our attention has now been drawn towards hydrolytic degradation processes at 37 °C and different pH values, from acidic to basic conditions, as in the GIT. For that, two sets of branched and linear D-mannitol-based polyurethanes containing disulfide bonds have been synthesized, which has been possible depending on the starting D-mannitol-derived monomer. Thus 3,4-*O*-isopropylidene-D-mannitol, having two

secondary hydroxyl groups in addition to the two primary hydroxyl groups, afforded polyurethanes with a certain degree of branching. In contrast, 2,4:3,5-di-*O*-isopropylidene-D-mannitol and 2,3:4,5-di-*O*-isopropylidene-D-mannitol, lacking secondary hydroxyl groups, led to linear polyurethanes. Removal of the *O*-isopropylidene protecting groups resulted in more-hydrophilic materials. As in glutathione-mediated degradation, the branched polyurethanes presented enhanced degradation under physiological conditions, proportional to the content of D-mannitol, whereas linear polyurethanes were degraded slowly, and pH 8 and 10 were required.

Keywords:

Hydrophilic polyurethanes

Polyhydroxyurethanes

Physiological conditions

Hydrolytic degradation

Carbohydrate-based polyurethanes

Stimuli-responsive polymers

ACCEPTED MANUSCRIPT

1. Introduction

Achieving sustained degradable materials under neutral conditions is a multifaceted challenge. In the case of biomaterials, which are intimately related to physiological conditions, this interest is more pronounced since —besides being biodegradable— they must be biocompatible. Fortunately, tailor-made biomaterials with specific molecular requirements can today be designed and synthesized depending on the properties and applications that are needed [1]. Structural architecture, multifunctionality, or stimuli-responsiveness are, among others, relevant features of biomaterials for specific applications, and moreover, physicochemical and degradation properties may be critical. In this sense, degradable natural or synthetic polymers that are sensitive to aqueous or enzymatic hydrolysis are currently hot topics [2].

The recurring problem of low bioavailability in the systemic administration of drugs is being resolved by the development of advanced polymeric systems for drug delivery and release. Intelligent systems are capable of response under physiological stimuli, such as changes in pH or temperature, enzyme concentration, or redox gradients [3-6]. Nonetheless, degradability is one of the most important obstacles to surmount in order to avoid undesired effects and toxicity [7]. Hydrolytic degradation of polymers is less specific

than enzymatic degradation, but conversely the degradation rate is generally more constant, regardless of the part of the organism. For this purpose the design of polymeric structures containing labile organic functions is highly convenient [8,9].

With regard to cancer therapy, it is well known that the hypoxic tumor microenvironment is a potential contributor to cancer stem-cell evolution [10]. Specific drug carriers for cancer therapy should reach the proper target site and be able to deliver the specific drug by responding to the intrinsic reducing stimuli of that hypoxic microenvironment. Polymers containing disulfide bonds are among the most widely studied as drug carriers, since such bonds undergo thiol-disulfide exchange mediated by glutathione (GSH) in cells, with the consequent release of the drug [7,11-13]. Furthermore, metastatic cancer treatment may be conducted by controlling the redox state in cancer cells [14]. Success in reaching the therapeutic target —the tumor— depends on factors such as tunable release of drugs from carriers with controlled degradability, as well as bioconjugation processes, among others [15,16].

Since polyurethanes (PUs) can be synthesized under mild reaction conditions, a variety of functionalized PUs are available with labile organic functional groups, conferring on them a low-toxic character. Additionally, synthetic carbohydrate-based polyurethanes

obtained from easily accessible monosaccharides [17-19] by either hydrolytic or enzymatic processes [20-25] are biocompatible and degradable materials. Those PUs containing disulfide bonds and carbohydrate moieties in the backbone repeating units were degraded by GSH [22-25]. It was demonstrated that a pair of structural properties such as the degree of crystallinity and hydrophilicity of these materials are of relevance for degradation rate. Hydrophilicity is an essential factor for biodegradation as well as for the hydrolytic degradation of synthetic polymeric materials, especially under mild conditions such as the physiological ones. In this sense, polymers with tunable hydrophilicity are of great interest for biomedical applications [26-28].

We have synthesized a variety of redox-sensitive PUs and copolyurethanes (CoPUs) containing disulfide bonds and D-mannitol –as carbohydrate moiety– in the polymer chains. The hydrophilic nature of these materials was provided by different D-mannitol monomers, containing one or two *O*-isopropylidene protecting groups (IM and DIM respectively). The hydrophilic character of these materials was enhanced by removal of these acetal groups. We have recently demonstrated the potential use of a PU based on IM for sustained drug release in the gastrointestinal tract [29]. Additionally we have published the capacity of different PUs and coPUs based on

IM, with diverse degree of hydrophilicity, to modulate the glutathione response [30]. We demonstrated that the inherent hydrophilicity of these materials was a crucial factor in explaining the scope of this kind of degradation, the most-hydrophilic materials with the highest content in D-mannitol being the fastest to be degraded. We now present the results on the hydrolytic degradation studies at 37 °C, under different pH values: 2, 7, 8 and 10. We have observed that the more-hydrophilic branched polyurethanes were hydrolytically degraded more widely under the conditions studied, which included physiological conditions.

2. Experimental part

2.1. Materials

The following commercial reagents were purchased from Sigma-Aldrich Co. St. Louis, MO, USA, and they were used as received without further purification: Dibutyltin dilaurate (DBTDL, 95%), D-mannitol (≥98%), 2,2′-dithiodiethanol (DT, Technical grade), 3,3′-dithiodipropionic acid (99%), hydrazine monohydrate (64-65% water solution, reagent grade 98%).

The following buffer solutions were used: Buffer solution pH 2.00 (20 °C) (citric acid, sodium hydroxide, hydrogen chloride, Scharlab S.L., Sentmenat, Spain), Buffer solution pH 7.00 (20 °C) (99%, potassium

di-hydrogen phosphate, di-sodium hydrogen phosphate 12 hydrate, Panreac, Darmstadt, Germany), Buffer solution pH 8.00 (20 °C) (99.99%, boric acid, potassium chloride, sodium hydroxide, Scharlab S.L, Sentmenat, Spain), Buffer solution pH 10.00 (20 °C) (99.98%, sodium carbonate, sodium hydrogen carbonate, Scharlab S.L., Sentmenat, Spain).

The solvents used for purification and characterizations were of technical or high-purity grade, which were purchased from Merck (Darmstadt, Germany), and they were dried when necessary by the use of molecular sieves (Scharlab S.L., Sentmenat, Spain).

2.2. General methods

The polymerization reaction assays were performed in the absence of humidity, under an inert atmosphere. All glassware was heated overnight at 80 °C before use. The pure monomers were dried under vacuum and stored under an inert atmosphere until required.

IR spectra were recorded on a JASCO FT/IR-4200 spectrometer equipped with ATR.

^{1}H and ^{13}C NMR spectra were recorded in the laboratories of the CITIUS Service of the University of Seville, using a Bruker AV-300 or a Bruker Advance AMX-500, or in the Polytechnic University

of Catalonia (UPC), using a Bruker AMX-300 apparatus. Chemical shifts (δ) are reported as parts per million downfield from tetramethylsilane (Me_4Si). Two-dimensional shift correlation spectra, such as ^{1}H-^{1}H homonuclear and ^{13}C-^{1}H heteronuclear, were also recorded with the COSY and HETCOR pulse sequences respectively.

Molecular weights were determined by gel permeation chromatography (GPC), using Waters equipment provided with a refractive-index detector 2414 (thermostatted at 40 °C). *N,N*-dimethylformamide (DMF) containing LiBr (5.8 mM solution) was the mobile phase. Samples (100 µL of 0.1% (w/v) solution) were injected and chromatographed with a flow of 1 mL min^{-1}. HR3 and HR4 Waters Styragel columns (7.8 x 300 mm) were used, linked in series and protected with a guard column, thermostatted at 60 °C. Molar mass averages and their distributions were estimated against polystyrene standards.

The thermal behavior of the polyurethanes was examined by differential scanning calorimetry (DSC) using a TA DSC Q200 Instrument calibrated with indium. Samples of about 2-3 mg were heated at a rate of 10 °C min^{-1} under a nitrogen flow of 50 mL min^{-1}, and cooled to -35 °C. The melting temperature (T_m) was taken as the maximum of the endothermic peak appearing on heating traces

recorded at 10 °C min^{-1}, and the glass transition temperature (T_g) was taken as the temperature for the inflection point seen on heating traces recorded at 20 °C min^{-1} from samples quenched from the melt. Thermogravimetric analyses (TGA) were performed with a TA SDT Q600 thermobalance. Polymer samples with a weight of around 3-4 mg were heated at a rate of 10 °C min^{-1} within the temperature range of 30-600 °C under an inert atmosphere.

Scanning electron microscopy (SEM) images were taken with a field emission DUAL BEAM AURIGA (ZEISS) instrument. The samples were coated with gold using a Leica DC500 instrument.

2.3. Synthesis of monomers

Monomers 2,4:3,5-di-*O*-isopropylidene-D-mannitol (DIMA) and 2,3:4,5-di-*O*-isopropylidene-D-mannitol (DIMB) [31] and dithiodiethyldiisocyanate (DI) [32] were obtained according to the corresponding described procedures. Spectroscopic characterization of monomers DIMA and DIMB is described in Appendix A (Supplementary data).

2.4. General procedure for the synthesis of polyurethanes and copolyurethanes

The branched IM-based polyurethanes were synthesized and characterized in detail as we have already described [30]. These polymers were used in this work for hydrolytic degradation studies and also for studies of controlled release of model drugs. The aforementioned synthetic procedure has now been extended to the preparation of linear DIM-based polyurethanes. The general synthetic procedure is summarized as follows: the selected alditol [3,4-*O*-isopropylidene-D-mannitol (IM), 2,4:3,5-di-*O*-isopropylidene-D-mannitol (DIMA), or 2,3:4,5-di-*O*-isopropylidene-D-mannitol (DIMB)] was made to react with dithiodiethyldiisocyanate (DI) in the presence of dibutyltin dilaurate (DBTDL) as catalyst. In the case of coPUs of IM, 2,2'-dithiodiethanol (DT) in the adjusted molar ratio was incorporated into the reaction medium. Thus, PUs, namely PU(IM-DI], PU(DIMA-DI, PU(DIMB-DI), and coPUs PU(IM_xDT_yDI), were obtained as white solid materials in average 80% yield.

2.4.1. Synthesis and structural characterization of Linear PU(DIMA-DI) and Linear PU(DIMB-DI)

Both linear PUs were obtained as follows.

A round-bottom flask was loaded with 4 mmol of the corresponding diol monomer, 2,4:3,5-di-*O*-isopropylidene-D-mannitol

(DIMA) or 2,3:4,5-di-*O*-isopropylidene-D-mannitol (DIMB), and it was subjected to three cycles of vacuum-argon. Then dry THF (4 mL) was added to get a solution, to which dithiodiethyldiisocyanate (DI) (4 mmol) was added under stirring, followed by the catalyst DBTDL (0.2%-mole relative to the monomers). Stirring was continued under argon atmosphere at room temperature for 24 h. Finally, the reaction mixture was treated with *tert*-butyl alcohol (1.2 mL) for 30 min, and added dropwise into cold *tert*-butyl methyl ether (200 mL). The precipitated polymer was filtered, washed with more ether, and dried under vacuum at 40 °C for 24 h to afford the title PUs as white solid materials in 80 and 82% yields, respectively.

Data concerning physicochemical characterization *of* Linear PU(DIMA-DI):

GPC: M_w 74,100; M_n 48,700; M_w/M_n 1.5.

IR: ν_{max} (cm^{-1}) 1698 (C=O urethane), 1524 (N-H urethane), 1217 (N-CO-O).

^{1}H NMR (DMSO-d_6, 500 MHz), δ (ppm): 1.22, 1.28 [2s, 12H, 2 $C(CH_3)_2$], 2.69-2.82 (m, 4H, 2 CH_2S), 3.19-3.30 (m, 4H, 2 CH_2NH), 3.68-3.77 (m, 2H, H-3, H-4), 3.78-3.83 (m, 2H, H-2, H-5), 3.96-4.14 (m, 4H, H-$1_{a,b}$, H-$6_{a,b}$), 7.36 (br s, 2H, 2 NH). $^{13}C\{^1H\}$-NMR (DMSO-d_6, 125 MHz), δ (ppm): 23.6, 24.4 [2 $C(CH_3)_2$], 37.5 (CH_2S), 39.7

(CH_2NH), 63.7 (C-1, C-6), 67.5 (C-2, C-5), 68.0 (C-3, C-4), 100.5 [*C*$(CH_3)_2$], 156.0 (CO).

Data concerning physicochemical characterization of Linear PU(DIMB-DI):

GPC: M_w 57,000; M_n 41,800; M_w/M_n 1.4.

IR: ν_{max} (cm^{-1}) 1699 (C=O urethane), 1523 (N-H urethane), 1216 (N-CO-O).

^{1}H NMR (DMSO-d_6, 500 MHz), δ (ppm): 1.28, 1.39 [2s, 12H, 2 C$(CH_3)_2$], 2.69-2.82 (m, 4H, 2 CH_2S), 3.19-3.38 (m, 4H, 2 C*H*$_2$NH), 3.95-4.04 (m, 2H, H-1_a, H-6_a), 4.11-4.19 (m, 2H, H-1_b, H-6_b), 4.19-4.27 (m, 2H, H-2, H-5), 4.28-4.37 (m, 2H, H-3, H-4), 7.37 (br s, 2H, NH). ^{13}C{^{1}H}-NMR (DMSO-d_6, 125 MHz), δ (ppm): 25.2, 27.0 [2 C(*C*$H_3)_2$], 37.4 (CH_2S), 39.9 (CH_2NH), 63.5 (C-1, C-6), 74.1 (C-2, C-5), 74.8 (C-3, C-4), 108.1 [2 *C*$(CH_3)_2$], 155.9 (CO).

2.5. Removal of the O-protecting isopropylidene groups of the polyurethanes

2.5.1. PU(M-DI) and PU(M_xDT_yDI)

These hydroxylated polyurethanes and copolyurethanes have been previously synthesized [30].

2.5.2. Linear PU(MA-DI) and Linear PU(MB-DI)

A suspension of Linear PU(DIMA-DI) or Linear PU(DIMB-DI) (350 mg, 0.75 mol) in THF (2 mL) was stirred with a mixture of TFA/H_2O 6:1 (2.3 mL) at room temperature for 3 hours. Then the reaction mixture was added dropwise into cold *tert*-butyl methyl ether (250 mL) while stirring. The precipitated polymer was filtered, washed with more ether and dried under vacuum for 24 hours to afford the title polyurethanes in 82 and 88% yields, respectively.

Data concerning physicochemical characterization of Linear PU(MA-DI):

GPC: M_w 94,200; M_n 65,100; M_w/M_n 1.4.

IR: ν_{max} (cm^{-1}) 3320 (N-H, O-H), 1687 (C=O urethane), 1541 (N-H urethane), 1261 (N-CO-O).

^{1}H NMR (DMSO-d_6, 500 MHz), δ (ppm): 2.69-2.91 (m, 4H, 2 CH_2S), 3.17-3.35 (m, 4H, CH_2NH), 3.43-3.74 (m, 4H, H-2, H-3, H-4, H-5), 3.69 (br s, 4H, 4 OH), 3.84-3.99 (m, 2H, H-1_a, H-6_a), 4.11-4.30 (m, 2H, H-1_b, H-6_b), 7.22 (br s, 2H, 2 NH). $^{13}C\{^1H\}$-NMR (DMSO-d_6, 125 MHz), δ (ppm): 37.4 (CH_2S), 39.7 (CH_2NH), 67.1 (C-1, C-6), 68.8 (C-2, C-5), 69.1 (C-3, C-4), 156.8 (CO).

Data concerning physicochemical characterization of Linear PU(MB-DI):

GPC: M_w 66,500; M_n 46,900; M_w/M_n 1.4.

IR: ν_{max} (cm^{-1}) 3318 (N-H, O-H), 1686 (C=O urethane), 1541 (N-H urethane), 1261 (N-CO-O).

^{1}H NMR (DMSO-d_6, 500 MHz), δ (ppm): 2.71-2.83 (m, 4H, 2 CH_2S), 3.23-3.31 (m, 4H, 2 CH_2NH), 3.50-3.58 (m, 2H, H-3, H-4), 3.59-3.83 (m, 6H, H-2, H-5, 4 OH), 3.88-3.96 (m, 2H, H-1_a, H-6_a), 4.20-4.27 (m, 2H, H-1_b, H-6_b), 7.21 (br s, 2H, 2 NH). ^{13}C{^{1}H}-NMR (DMSO-d_6, 125 MHz), δ (ppm): 37.4 (CH_2S), 39.7 (CH_2NH), 67.1 (C-1, C-6), 68.8 (C-2, C-5), 69.1 (C-3, C-4), 156.7 (CO).

2.6. Hydrolytic degradation studies

Preparation of polymer disks. The disks were prepared by the application of pressure (10 ton/cm^2) on powdered samples (20 ± 5 mg) for 5 min at 25 °C. These disks were dried under vacuum at 40 °C for 48 h.

Degradation conditions. For the hydrolytic degradation studies, each polymer disk (160 ± 10 µm in thickness) was immersed in a vial containing 5 mL of one of the following buffer solutions: citrate buffer pH 2.00, phosphate buffer pH 7.00, borate buffer pH 8.00, or

carbonate buffer pH 10.00. The vials were then sealed and heated at 37 ± 0.5 °C for a specific period of time. In the case of incubation at pH 7.00, the disks were submerged in the corresponding buffer solution and heated at 37 ± 0.5 °C while stirring with an orbital stirrer (200 rpm). At the end of the scheduled incubation periods, the disks were withdrawn from the incubation medium, washed thoroughly with distilled water, dried to constant weight, and then subjected to GPC analysis.

3. Results and discussion

3.1. Synthesis and chemical structure

As mentioned above the synthesis and characterization of branched PUs and coPUs based on 3,4-*O*-isopropylidene-D-mannitol (IM) and 2,2'-dithiodiethanol (DT) as monomer diols, and dithiodiethyldiisocyanate (DI) has previously been reported by us [29,30]. We now describe the preparation of linear PUs starting from 2,4:3,5-di-*O*-isopropylidene-D-mannitol (DIMA) and 2,3:4,5-di-*O*-isopropylidene-D-mannitol (DIMB) and DI. Both types of polyurethane were obtained by the same synthetic procedure, as shown in Schemes 1 and 2. They were all obtained as white solid materials in average 80% yield.

As we have already described, PUs and coPUs derived from IM, PU(IM-DI) and PU(IM_xDT_yDI), respectively, presented a certain degree of branching, as demonstrated by NMR studies. This was due to the reaction of some of the secondary hydroxyl groups of the IM monomer with the diisocyanate DI. The subscript x and y letters shown in the abbreviations, correspond to %molar ratio of the diols in the copolymer calculated by ^{1}H NMR, which were very close in all copolymers to the initial feed ratio. From the integration of the corresponding ^{1}H NMR spectra, 10% of branching was estimated for PU(IM-DI) and 16–20% for the coPUs.

However, in the case of PUs derived from di-*O*-isopropylidene monomers DIMA and DIMB, no branching is possible due to the absence of secondary hydroxyl groups, so linear PUs were obtained. Hence, these PUs are referred to as Linear PU(DIMA-DI) and Linear PU(DIMB-DI).The structural characterization of the monomers DIMA and DIMB is presented in Appendix A.

Removal of the *O*-isopropylidene protecting groups was accomplished by hydrolysis with TFA in THF-water under different conditions, depending on the D-mannitol moiety present in the polymer chains (Schemes 3 and 4). Thus, in the case of the isopropylidene groups of PU(IM-DI) and PU(IM_xDT_yDI), warming the reaction mixtures at 40-45 °C overnight was necessary. In contrast,

the diisopropylidene groups of PU(DIMA-DI) and PU(DIMB-DI) were more easily removed —stirring at room temperature for 3 h was sufficient. The new polyhydroxyurethanes were named as Linear PU(MA-DI) and Linear PU(MB-DI).

3.2. Thermal properties

The thermal behavior of the polyurethanes that were going to be degraded has been comparatively examined by TGA and DSC; the parameters resulting from this study are shown in Tables 1 and 2. The thermal data of PU(IM-DI) and its coPUs PU($M_{81}DT_{19}$DI) and PU($M_{48}DT_{52}$DI), as well as their polyhydroxy derivatives [30], has been included for comparative purposes in order to correlate the thermal properties and the hydrodegradability behaviour. In addition to this, TGA and DSC traces of partially branched PU(IM-DI), Linear PU(DIMA-DI), and Linear PU(DIMB-DI), and their corresponding polyhydroxy derivatives, are shown in Fig. 1 and 2 respectively.

The TGA traces for the *O*-protected PUs recorded under an inert atmosphere presented a similar pattern of decomposition behavior (Table 1, and Fig. 1a). The partially branched PU(IM-DI) presented thermal decomposition starting to be detectable at about 258 °C, with onset temperatures (measured for 10% of weight loss) between 258 °C and 279 °C. For Linear PU(DIMA-DI) and Linear

PU(DIMB-DI) the thermal decomposition was very similar: in the range 260-280 °C and 262-275 °C respectively. The decomposition processes found for all of them took place in a single stage following an identical profile, with maximum degradation rate in the range 275-280 °C, and a residue below 9% of the initial weight.

The DSC studies showed no melting transition temperature for PU(IM-DI), but a thermal transition corresponding to a T_g was observed at 67 °C, which confers an amorphous character to this material. In contrast, the coPUs PU($IM_{81}DT_{19}DI$) and PU(IM_{48}-$DT_{52}DI$) were semicrystalline materials [30] (see also Table 1) whose T_g values decreased with the content of IM.

On the other hand, linear PUs based on DIM were amorphous materials. Linear PU(DIMA-DI) and Linear PU(DIMB-DI) presented T_g values of 90 ºC and 81 °C respectively. This difference of 9 °C in T_g can be explained as a function of the different stiffness provided by the nature of the isopropylidene acetal groups of DIMA and DIMB monomers; DIMA has two fused 6-member rings and is a rigid monomer, while DIMB has two independent 5-member rings and is quite a flexible monomer. These structural features present in the repetitive constitutional units confer a different degree of stiffness on the polymer chains, depending on the starting monomer.

The *O*-deprotected Linear PU(MA-DI) and Linear PU(MB-DI) were semicrystalline materials. From TGA measurements (Table 2 and Fig. 1b) we found that the linear PUs started thermal decomposition with onset temperatures (measured for 10% of weight loss) between 210 °C and 214 °C. The decomposition profile presented a single stage, with maximum degradation rate in the range 244-246 °C and a residue below 4% of the initial weight. Thus the maximum degradation rate is 15 °C and 17 °C lower than that observed for the partially branched PU(M-DI).

The DSC studies (Table 2 and Fig. 2b) revealed lower glass transition temperatures for all the polyhydroxy derivatives compared with their acetalized counterparts. Thus the DSC traces of Linear PU(MA-DI) and Linear PU(MB-DI), showed T_g values of 40 °C and 30 °C, respectively, which means a 50% decrease with respect to the acetalized parent polymers. The observed difference in T_g can be attributed to the different molecular weights of the two linear polyhydroxy derivatives. In the case of PU(M-DI), a T_g of 59 °C was observed —this is 8 °C lower than its corresponding starting *O*-protected PU.

The DSC thermograms for these PUs showed endothermic transitions of melting. Despite the branched PU(IM-DI) having an amorphous character, its corresponding PU(M-DI) showed a main T_m

at 122 °C, (□H_m= 26 J g^{-1}). All the coPUs, and their polyhydroxy coPUs PU($M_{81}DT_{19}DI$) and PU($M_{48}DT_{52}DI$), were semicrystalline materials [30] (Table 2), their T_g decreasing with the content of mannitol.

The T_m of Linear PU(MA-DI) and PU(MB-DI) were 163 ºC and 158 ºC respectively, and the peaks associated to crystallization processes were observed at 138 °C and 121 °C respectively (Table 2).

To sum up, all the polyhydroxy-PUs and -coPUs were semicrystalline materials and presented lower T_g than their acetalized parent materials, independently of the branched or linear structure. All branched polyurethanes and copolyurethanes were observed to be less crystalline than the linear ones, with both melting temperatures and enthalpies being lower as a consequence of these branches making it difficult for the polymer molecules to pack in a regular array.

3.3. Hydrolytic degradation studies

We had previously studied the degradation of a selected set of disulfide-bond-containing homoPUs PU(IM-DT) and co-polyurethanes PU(IM_x-DT_yTDI) by the action of the bio-redox regulator glutathione (GSH) [30]. We demonstrated that the

glutathione-mediated degradation of those materials showed how the ratio of hydroxyl to disulfide groups modulates the response of GSH under physiological conditions, and it was seen that the inherent hydrophilicity of each of them plays a determining role in this kind of degradation process.

In the case of hydrolytic degradation, hydrophilicity also plays a very important role. Hydrophilicity is intimately related to water absorption and this is a key parameter to be taken into account, since hydrolysis of the urethane function is the chemical reaction responsible for degradation in this kind of polymer [34]. We now report on the hydrolytic degradation studies of the above-mentioned polyurethanes under different pH conditions: pH 2.00, 7.00, 8.00, and 10.00 —hereinafter pH 2, 7, 8 and 10— with incubation at 37 °C. GPC was used to follow the hydrolytic processes by the decrease in molecular weight of the corresponding materials.

First, hydrolytic degradation of those PUs based on IM, such as PU(IM-DI), PU($IM_{81}DT_{19}DI$), and PU($IM_{48}DT_{52}DI$), was carried out at pH 7. The process was monitored for an exact period of time: 7, 14, 21, 28, 35, and 70 days. The degradation process is shown in Fig. 3, where remaining molecular weight (M_w) is plotted *versus* time. It can be seen that the degree of degradation increases with the content in D-mannitol as either IM or M, especially with M. Thus

PU(IM-DI) lost approx. 20% of its original M_w after 28 days of incubation, and its polyhydroxyl derivative PU(M-DI) presented a loss of 66% at that time. After 70 days of incubation they had lost approx. 55% and 76% of M_w, respectively.

In parallel, the same polymers cited in the previous paragraph were assayed at pH 2, pH 8, and pH 10 at 37 °C for 28 days; the results are plotted in Fig. 4. Once again the samples that degraded to a higher degree, in any range of pH values, were those with the highest content of IM or M in their polymeric chains. Such PUs were the most hydrophilic, and the fastest to be degraded. The chemical constitution of the different PUs and coPUs was consistent with the obtained results. As expected, all the PUs degraded to a greater extent under basic pH. For instance, PU(M-DI) —with the highest content in D-mannitol— lost 13.4% of M_w at pH 2. PU(IM-DI) and PU($IM_{81}DT_{19}DI$) lost approx. 30-37% of M_w at pH 8, with a 35% loss of M_w at pH 10. The corresponding polyhydroxy derivatives presented a similar pattern of M_w loss, losing up to 28-37% at pH 8, and 38-40% at pH 10. It is worth noting that this set of PUs and coPUs based on IM and their polyhydroxy derivatives were very hygroscopic, as we had previously verified [30], which favored the hydrolytic degradation [34]. As can be observed, the loss of M_w in these PUs and coPUs based on IM was higher at pH 7 than under

basic pH, which can be explained as due to the enhanced effect caused by stirring.

On the other hand, Linear PU(DIMA-DI) and Linear PU(DIMB-DI), as well as their corresponding *O*-deprotected derivatives, presented the same profile of degradation but to a lesser degree than their branched homologues (Fig. 5 and 6). In general, those PUs with higher content in D-mannitol lost up to 20-25% in M_w after incubation at pH 10 for 28 days. The difference in hygroscopicity as a consequence of differences in crystallinity between the non-linear and linear polyhydroxyurethanes could explain the greater degradation of the former, which were less crystalline.

Selected ^{1}H NMR spectra of the samples corresponding to the *O*-deprotected PU(M-DI) and Linear PU(MB-DI) recovered from the incubated media are shown in the Supplementary data. Detection of any amino or hydroxyl terminal groups proceeding from the hydrolysis of the urethane functions —especially for PU(M-DI)— is not so clear, probably due to the presence of abundant hydroxyl groups, including those already present in the parent acetalized material. For Linear PU(MB-DI), terminal hydroxymethyl groups can be observed at δ 4.75 ppm (Fig. S2).

SEM micrographs of polyhydroxy PU(M-DI), Linear PU(MA-DI), and Linear PU(MB-DI) before and after the incubation processes (Fig. 7 and 8) clearly demonstrate the traces of degradation. They all show that the degradation took place on the surface of the disks; thus Fig. 7 shows the erosive process on PU(M-DI), at 37 ºC and pH 7 for 70 days. Likewise, SEM micrographs of PU(M-DI), Linear PU(MA-DI), and Linear PU(MB-DI) demonstrate the erosion process on their respective surfaces at pH 10 for 28 days (Fig. 8).

Finally we can sum up that for hydrolytic degradation at different pH conditions —from pH 2 to pH 10— the presence of D-mannitol in the polymer chains is of relevance because it ensures the degradation process. Certain structural features, such as linearity or branching in the polymer chains, together with the presence of hydroxyl groups along them, are also important. Of the monomers IM and DIM, the polyurethanes originated from the former were the most hydrolytically degraded because they presented a certain degree of branching and were less crystalline and very hygroscopic materials. In general, all the polyhydroxy PUs studied here display low T_g values, which —together with the above-mentioned properties— enhances any kind of degradation process in comparison with the acetalized starting materials.

4. Conclusions

A variety of D-mannitol-based polyurethanes have been synthesized, structurally characterized, and subjected to hydrolytic degradation assays under conditions of pH (2, 7, 8 and 10) and temperature (37 ºC) typical of those in the gastrointestinal tract. They were all degraded to an extent depending on their structural constitution and thermal properties. The confluence of certain factors is determinant for an effective degradation: namely hydrophilicity, crystallinity, and glass transition temperature close to 37 °C. Thus the more-hydrophilic materials based on IM, and their corresponding polyhydroxy derivatives, with some degree of branching, presented an enhanced degradation progression. All the *O*-deprotected PUs had T_g values in the range 30-59 °C, which favored degradation at the physiological temperature. SEM studies confirmed the degradation effect mainly at the surface level of the studied sample disks at pH 7 and pH 10, depending on the substrate. Hopefully, continuing investigations of these materials will achieve their applicability as drug transporters in the gastrointestinal tract.

Acknowledgements

This work was supported by the Ministerio de Economía y Competitividad of Spain (MINECO) [Grant numbers MAT2012-

38044C03-01, MAT2016-77345-C3-2-P] and Junta de Andalucía [Grant number FQM-1563]. The authors are also indebted to the MINECO for the pre-doctoral grant (FPI) awarded to Lucía Romero-Azogil.

Appendix A. Supplementary data

References

[1] S.-B. Park, E. Lih, K.-S. Park, Y.K. Joung, D.K. Han, Biopolymer-based functional composites for medical applications, Prog. Polym. Sci. 68 (2017) 77–105, https://doi.org/10.1016/j.progpolymsci.2016.12.003.

[2] K. Ginjupalli, G. Venkat Shavi, R. Kumar Averineni, M. Bhat, N. Udupa, P. Nagaraja Upadhya, Poly(□-hydroxy acid) based polymers: A review on material and degradation aspects. Polym. Degrad. Stab. 144 (2017) 520–535, http://dx.doi.org/10.1016/j.polymdegradstab.2017.08.024.

[3] Y. Zhang, H.F. Chan, K.W. Leong, Advanced materials and processing for drug delivery: The past and the future, Adv. Drug

Deliv. Rev. 65 (2013) 104–120, https://doi.org/10.1016/j.addr.2012.10.003.

[4] A.K. Bajpai, S.K. Shukla, S. Bhanu, S. Kankane, Responsive polymers in controlled drug delivery, Prog. Polym. Sci. 33 (2008) 1088–1118, https://doi.org/10.1016/j.progpolymsci.2008.07.005.

[5] S. Mura, J. Nicolas, P. Couvreur, Stimuli-responsive nanocarriers for drug delivery, Nat. Mater. 12 (2013) 991–1003, https://doi.org/10.1038/NMAT3776.

[6] P. Zhang, H. Zhang, W. He, D. Zhao, A. Song, Y. Luan, Disulfide-linked amphiphilic polymer-Docetaxel conjugates assembled redox-sensitive micelles for efficient antitumor drug delivery, Biomacromolecules, 17 (2016) 1621–1632, https://pubs.acs.org/doi/10.1021/acs.biomac.5b01758.

[7] G.K. Such, Y. Yan, A.P.R. Johnston, S.T. Gunawan, F. Caruso, Interfacing materials science and biology for drug carrier design, Adv. Mater. 27 (2015) 2278–2297, https://doi.org/10.1002/adma.201405084.

[8] M.F. Maitz, Applications of synthetic polymers in clinical medicine, Biosurf. Biotribol. 1 (2015) 161–176, https://doi.org/10.1016/j.bsbt.2015.08.002.

[9] L.S. Nair, C.T. Laurencin, Biodegradable polymers as biomaterials, Prog. Polym.Sci. 32 (2007) 762–798, https://doi.org/10.1016/j.progpolymsci.2007.05.017.

[10] A. Carnero, M. Lleonart, The hypoxic microenvironment: A determinant of cancer stem cell evolution, Inside the cell, 1 (2016) 96–105, https://doi.org/10.1016/j.bsbt.2015.08.002.

[11] J. Yang, Y. Duan, X. Zhang, Y. Wang, A. Yu, Modulating the cellular microenvironment with disulfide-containing nanoparticles as an auxiliary cancer treatment strategy, J. Mater. Chem. B, 4 (2016) 3868–3873, https://doi.org/10.1039/C6TB00847J.

[12] N. Casado, G. Hernández, H. Sardon, D. Mecerreyes, Current trends in redox polymers for energy and medicine, Prog. Polym. Sci. 52 (2016) 107–135, https://doi.org/10.1016/j.progpolymsci.2015.08.003.

[13] X. Wang, J. Zhang, R. Cheng, F. Meng, C. Deng, Z. Zhong, Facile synthesis of reductively degradable biopolymers using cystamine diisocyanate as a coupling agent, Biomacromolecules 17 (2016) 882–890, https://doi.org/10.1016/j.progpolymsci.2015.08.003.

[14] W.Y. Yang, L.Z. Zou, C.H. Huang, Y.L. Lei, Redox regulation of cancer metastasis: Molecular signaling and therapeutic opportunities, Dev. Res. 75 (2014) 331–341, https://doi.org/10.1002/ddr.21216.

[15] Q. Zhang, N. R. Ko, J. K. Oh, Recent advances in stimuli-responsive degradable block copolymer micelles: synthesis and controlled drug delivery applications, Chem. Comm. 48 (2012) 7542–7552, https://doi.org/10.1039/C2CC32408C.

[16] J. Yang, Y. Duan, X. Zhang, Y. Wang, A. Yu, Modulating the cellular microenvironment with disulfide-containing nanoparticles as an auxiliary cancer treatment strategy, J. Mater. Chem. B, 4 (2016) 3868–3873, https://doi.org/10.1039/C6TB00847J.

[17] J.A. Galbis, M.G. García-Martín, Synthetic polymers from readily available monosaccharides, Top. Curr. Chem. 295 (2010) 147–176, https://doi.org/10.1007.

[18] J.A. Galbis, M.G. García-Martín, M.V. de Paz, E. Galbis, Synthetic polymers from sugar-based monomers, Chem. Rev. 116 (2016) 1600–36, http://dx.doi.org/10.1021/acs.chemrev.5b00242.

[19] J.A. Galbis, M.G. García-Martín, M.-V. de Paz, E. Galbis, Bio-based Polyurethanes from Carbohydrate Monomers, in: F. Yilmaz (Ed.), Aspects of Polyurethanes, InTech. Rijeka, Croatia, 2017, pp. 155–192, http://dx.doi.org/10.5772/intechopen.69606

[20] C. Ferris, M.V. de Paz, F. Zamora, J.A. Galbis, Dithiothreitol-based polyurethanes. Synthesis and degradation studies, Polym. Degrad. Stab. 95 (2010) 1480–1487, https://doi.org/10.1016/j.polymdegradstab.2010.06.021.

[21] B. Begines, F. Zamora, E. Benito, M.G. García-Martín, J.A. Galbis, Conformationally restricted linear polyurethanes from

acetalized sugar-based monomers, J. Polym. Sci. Part A: Polym. Chem. 50 (2012) 4638–4646, https://doi.org/10.1002/pola.26293.

[22] M.V. de Paz, F. Zamora, B. Begines, C. Ferris, J.A. Galbis, Glutathione-mediated biodegradable polyurethanes derived from L-arabinitol, Biomacromolecules 11 (2010) 269–276, https://doi.org/10.1021/bm9011216.

[23] C. Ferris, M.V. de Paz, A. Aguilar-de-Leyva, I. Caraballo, J.A. Galbis, Reduction-sensitive functionalized copolyurethanes for biomedical applications, Polym. Chem. 5 (2014) 2370–2381, https://doi.org/10.1039/c3py01572f.

[24] B. Begines, F. Zamora, M.V. de Paz, K. Hakkou, J.A. Galbis, Polyurethanes derived from carbohydrates and cystine-based monomers, J. Appl. Polym. Sci. 132 (2015) 41304–41311, https://doi.org/10.1002/app.41304.

[25] B. Begines, M.V. de Paz, A. Alcudia, J.A. Galbis, Synthesis of reduction sensitive comb-like polyurethanes using click

chemistry, J. Polym. Sci. Part A: Polym. Chem. 54 (2016) 3888–3900, https://doi.org/10.1002/pola.28367.

[26] M.C. Koetting, J.T. Peters, S.D. Steichen, N.A. Peppas, Stimulus-responsive hydrogels: Theory, modern advances, and applications, Mater. Sci. Eng. R, 93 (2015) 1–49, https://doi.org/10.1016/j.mser.2015.04.001.

[27] M.K. Nguyen, E. Alsberg, Bioactive factor delivery strategies from engineered polymer hydrogels for therapeutic medicine, Progr. Polym. Sci. 39 (2014) 1235–1265, http://dx.doi.org/10.1016/j.progpolymsci.2013.12.001.

[28] J. Chen, R. Dong, J. Ge, B. Guo, P. X. Ma, Biocompatible, biodegradable, and electroactive polyurethane-urea elastomers with tunable hydrophilicity for skeletal muscle tissue engineering, ACS Appl. Mater. Interfaces 7 (2015) 28273–28288, http://dx.doi.org/10.1021/acsami.5b10829.

[29] M.D. Campiñez, E. Benito, L. Romero-Azogil, A. Aguilar-de-Leyva, M.G. García-Martín, J.A. Galbis, I. Caraballo, Development and characterization of new functionalized

polyurethanes for sustained and site-specific drug release in the gastrointestinal tract, Eur. J. Pharm. Sci. 100 (2017) 285–295, https://doi.org/10.1016/j.ejps.2017.01.017.

[30] L. Romero-Azogil, E. Benito, M.G. García-Martín, J.A. Galbis, Tunable hydrophilicity of redox D-mannitol-based polyurethanes modulates glutathione response, Eur. Polym. J. 94 (2017) 259–269, http://dx.doi.org/10.1016/j.eurpolymj.2017.07.012.

[31] K. Gawronska, Synthesis and conformations of 2,3:4,5- and 2,4:3,5-di-*O*-isopropylidene-D-mannitol, Carbohydr. Res. 176 (1988) 79–85.

[32] Y. Teramura, Y. Kaneda, H. Iwata, Islet-encapsulation in ultra-thin layer-by-layer membranes of poly(vinyl alcohol) anchored to poly(ethylene glycol)–lipids in the cell membrane. Biomaterials 28 (2007) 4818–4825, https://doi.org/10.1016/j.biomaterials.2007.07.050.

[33] S. Mondal, D. Martin, Hydrolytic degradation of segmented polyurethane copolymers for biomedical applications, Polym. Degrad. Stab. 97 (2012) 1553–1561,

https://doi.org/10.1016/j.polymdegradstab.2012.04.008.

ACCEPTED MANUSCRIPT

Figure captions

Fig. 1. Comparative curves of thermal degradation under inert atmosphere of the *O*-protected (a), and *O*-deprotected (b) polyurethanes. Weight (%) versus temperature.

Fig. 2. DSC heating traces of the *O*-protected (a) and *O*-deprotected (b) polyurethanes recorded under heating from quenched samples for T_g observation.

Fig. 3. Hydrolytic degradation of selected PU(IM_xDT_yDI) and PU(IM-DI] (a), and the corresponding *O*-deprotected PU(MxDTyDI) and PU(M-DI) (b). Remaining molecular weight is plotted versus time, incubation at 37 °C, and pH 7 for 70 days.

Fig. 4. Hydrolytic degradation of selected PU(IM_xDT_yDI) and PU(IM-DI) (a), and the corresponding *O*-deprotected PU(M_xDT_yDI) and PU(M-DI) (b). Remaining molecular weight is plotted versus time, incubation at 37 °C and pH 2, pH 8, and pH 10 for 28 days.

Fig. 5. Hydrolytic degradation of Linear PU(DIMA-DI) (a), and the corresponding *O*-deprotected Linear PU(MA-DI) (b). Remaining molecular weight is plotted versus time, incubation at 37 °C and different pH for 28 days.

Fig. 6. Hydrolytic degradation of Linear PU(DIMB-DI) (a), and the corresponding *O*-deprotected Linear PU(MB-DI) (b). Remaining molecular weight is plotted versus time, incubation at 37 °C and different pH for 28 days.

Fig. 7. SEM micrographs of PU(M-DI) before (a) and after (b) incubation at 37 °C, pH 7, 70 days.

Fig. 8. SEM micrographs of PU(M-DI) (top), Linear PU(MA-DI) (middle), and Linear PU(MB-DI) (bottom) before (a) and after (b) incubation at 37 °C, pH 10, 28 days.

ACCEPTED MANUSCRIPT

ACCEPTED MANUSCRIPT

Table 1

Thermal properties of protected *O*-isopropylidene polyurethanes

Polyurethane	TGA			DSC		
	T_d[a] (°C)	T_{ds}[b] (°C)	ΔW[c] (%)	T_g[d] (°C)	T_m[e] (°C)	ΔH_m[e] (J g^{-1})
Linear PU(DIMA-DI)	260	280	9	90		
Linear PU(DIMB-DI)	262	275	5	81		
PU(IM-DI)[f]	258	279	8	67		
PU($IM_{81}DT_{19}DI$)[f]	226	261	8	55	70/117	3/3
PU($IM_{48}DT_{52}DI$)[f]	254	269	8	34	68/100	4/14

[a] Temperature at which 10% weight loss was observed in the TGA traces recorded at 10 °C min^{-1}.
[b] Temperature for maximum degradation rate.
[c] Remaining weight at 600 °C.
[d] Glass transition temperature taken as the inflection point of the heating DSC traces of melt-quenched samples recorded at 20 °C min^{-1}.
[e] Melting temperature (T_m) and respective enthalpy (ΔH_m) measured by DSC at a heating rate of 10 °C min^{-1}.
[f] Data corresponding to these PUs were taken from reference [30].

Table 2

Thermal properties of polyhydroxyurethanes.

Polyurethane	TGA			DSC				
	T_d[a](°C)	T_{ds}[b](°C)	ΔW[c](%)	T_g[d](°C)	T_m[e](°C)	ΔH_m[e](J g^{-1})	T_c[f](°C)	ΔH_c[f](J g^{-1})
Linear PU(MA-DI)	210	244	0	40	163	51	138	19
Linear PU(MB-DI)	214	246	4	30	158	52	121	13
PU(M-DI)[g]	231	261	9	59	90/122	4/26		
PU(M_{81}-DT_{19}DI)[g]	229	266	7	47	75/115	6/12		
PU(M_{48}-DT_{52}DI)[g]	232	242	19	13	110	37		

[a] Temperature at which 10% weight loss was observed in the TGA traces recorded at 10 °C min^{-1}.
[b] Temperature for maximum degradation rate.
[c] Remaining weight at 600 °C.
[d] Glass-transition temperature taken as the inflection point of the heating DSC traces of melt-quenched samples recorded at 20 °C min^{-1}.
[e] Melting temperature (T_m) and respective enthalpie (ΔH_m) measured by DSC at a heating rate of 10 °C min^{-1}.
[f] Crystallization (T_c) temperature and respective enthalpie (ΔH_c) measured by DSC at a heating rate of 10 °C min^{-1}
[g] Data corresponding to these PUs were taken from reference [30].

ACCEPTED MANUSCRIPT

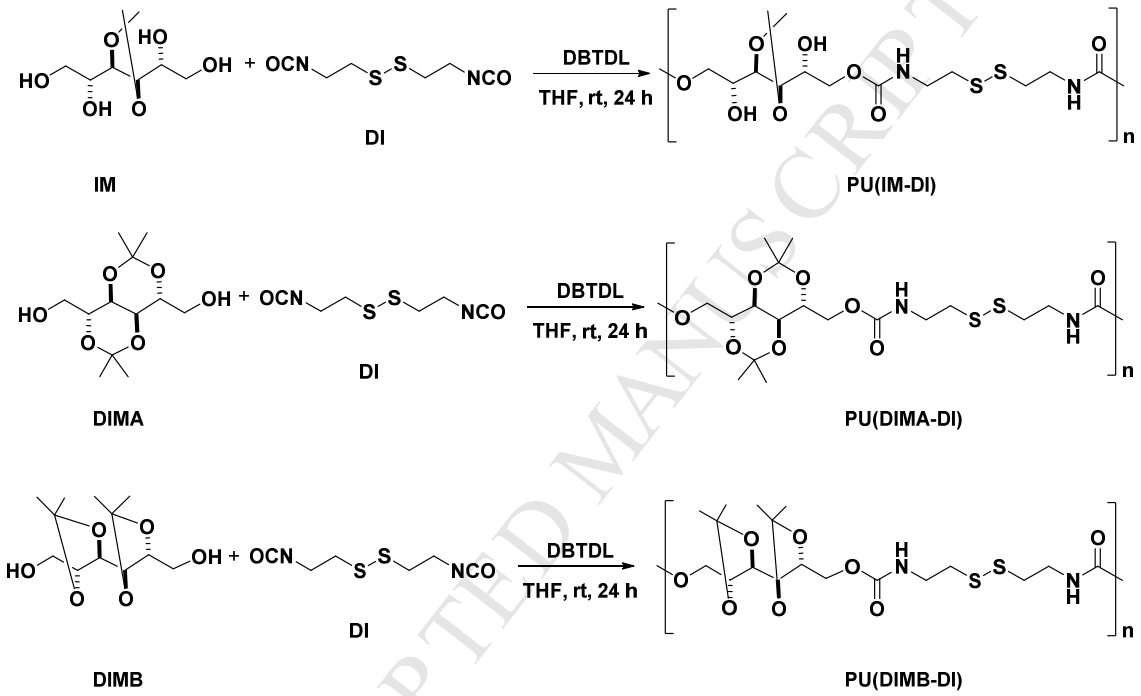

Scheme 1. Polyaddition reactions leading to homopolyurethanes.

ACCEPTED MANUSCRIPT

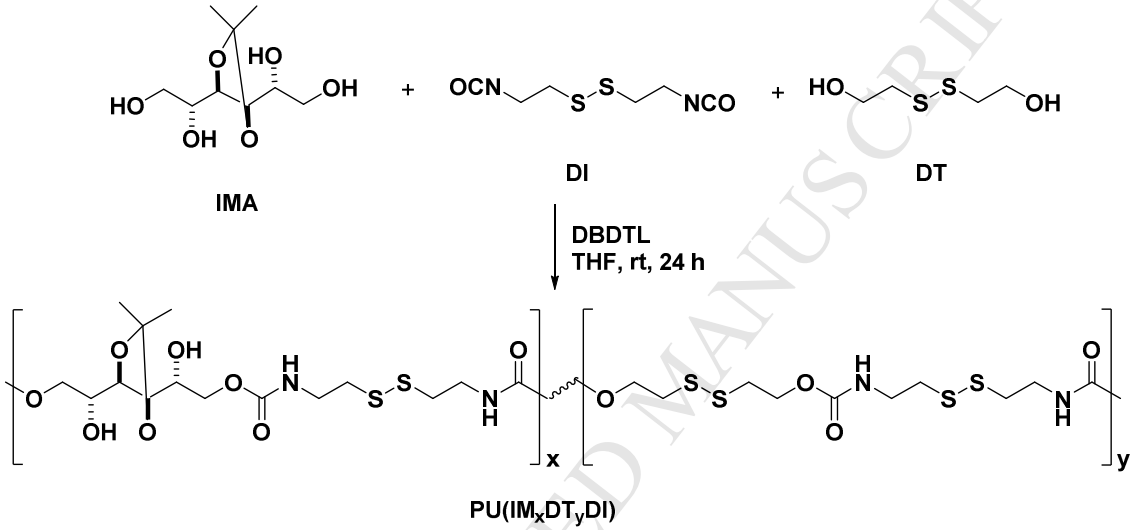

Scheme 2. Polyaddition reactions leading to copolyurethanes.

ACCEPTED MANUSCRIPT

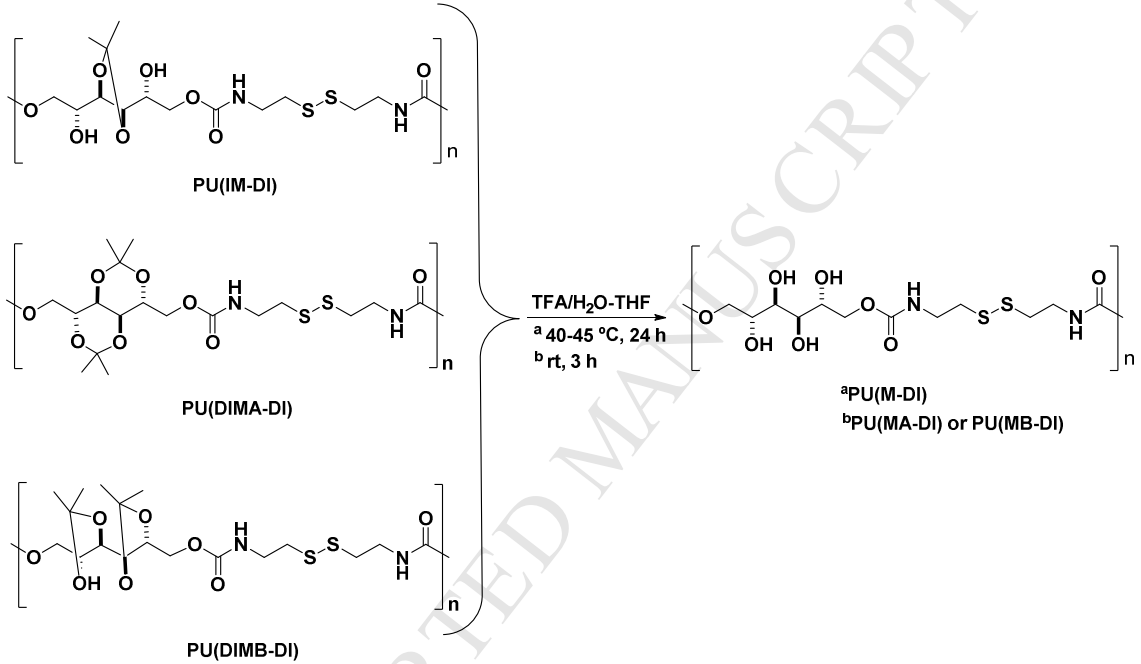

Scheme 3. Polyhydroxyurethanes from their parent PUs by removal of the *O*-isopropylidene groups.

ACCEPTED MANUSCRIPT

ACCEPTED MANUSCRIPT

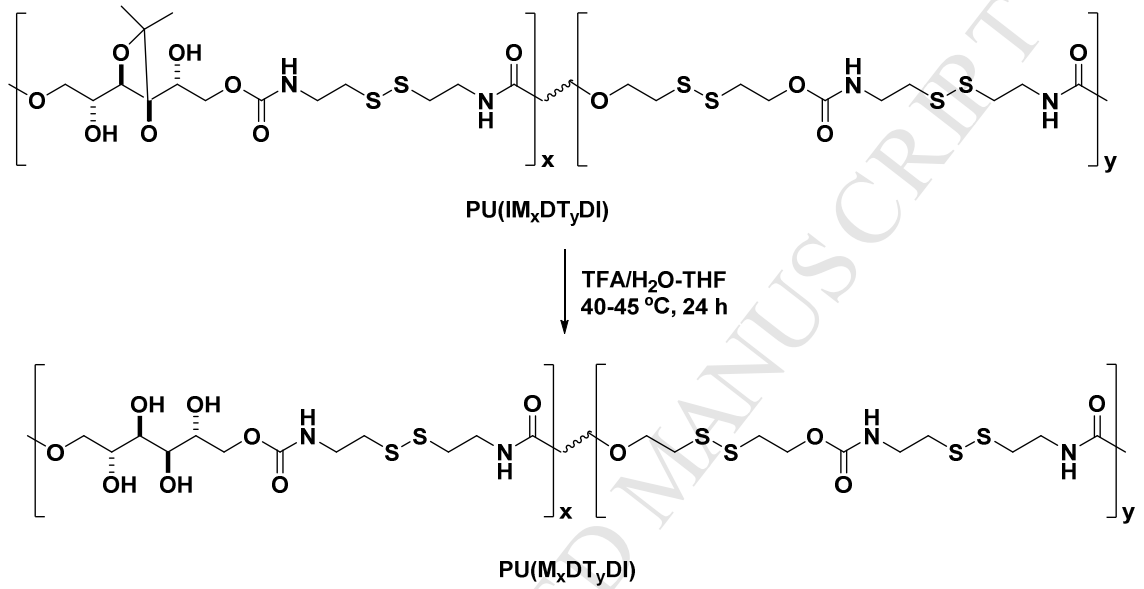

Scheme 4. Copolyhydroxyurethanes from their parent coPUs by removal of the *O*-isopropylidene groups.

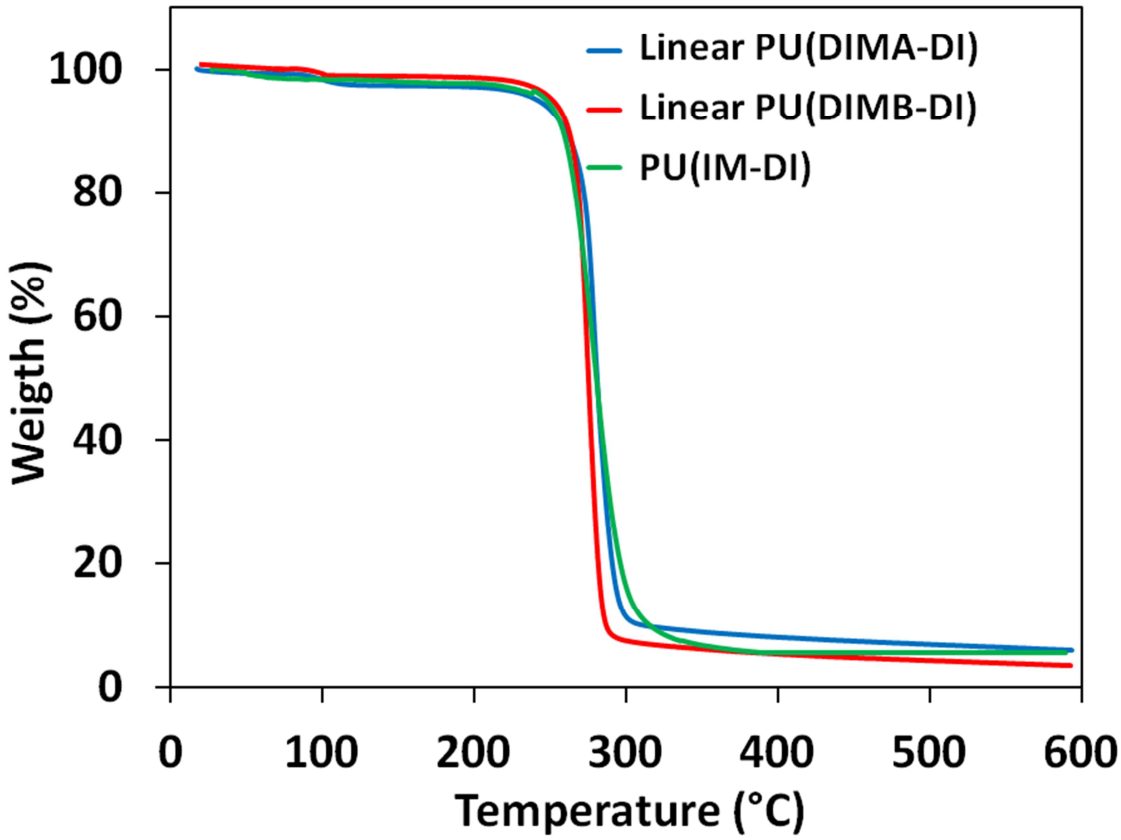

ACCEPTED MANUSCRIPT

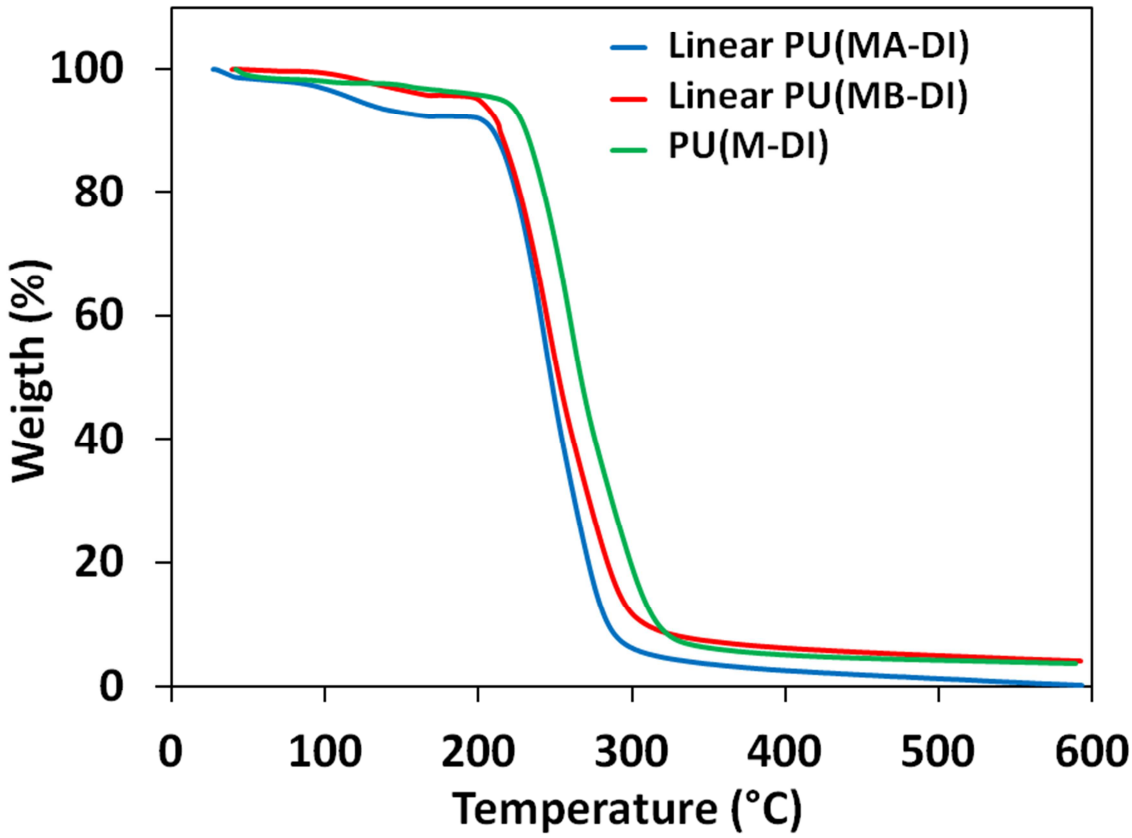

ACCEPTED MANUSCRIPT

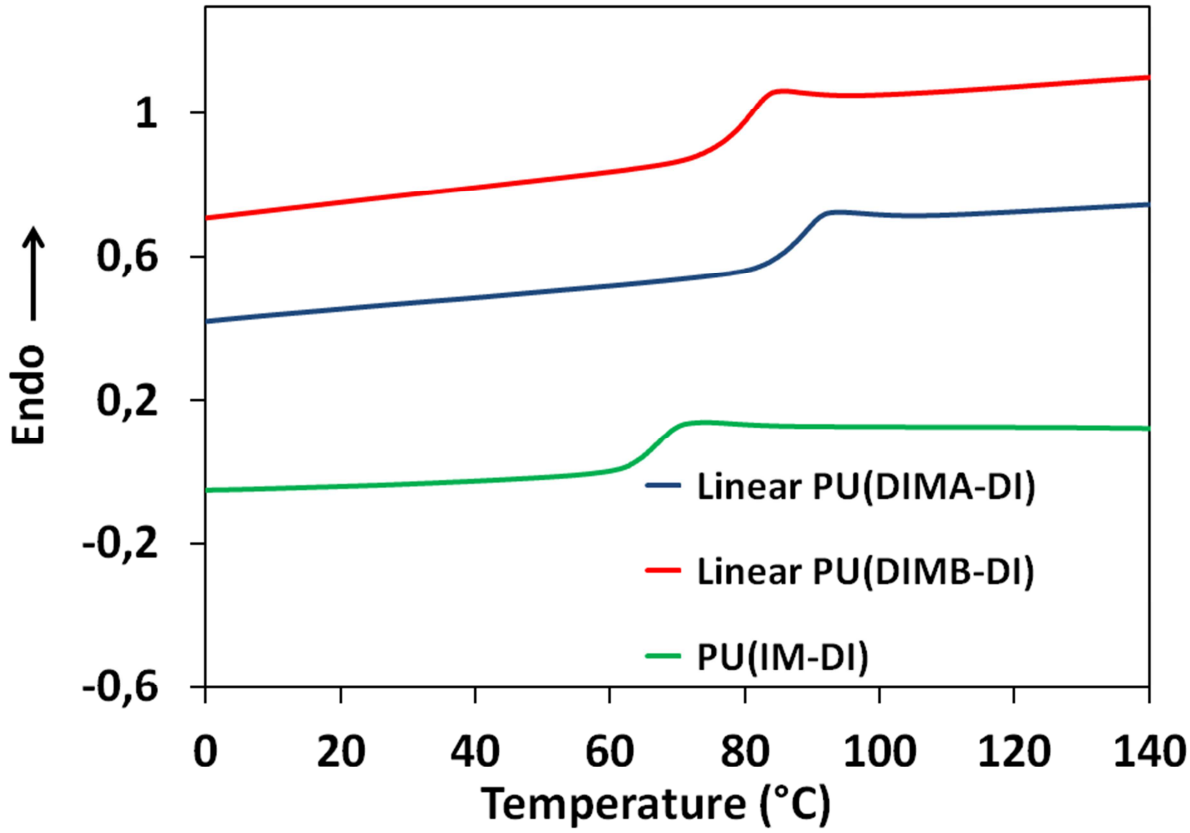

ACCEPTED MANUSCRIPT

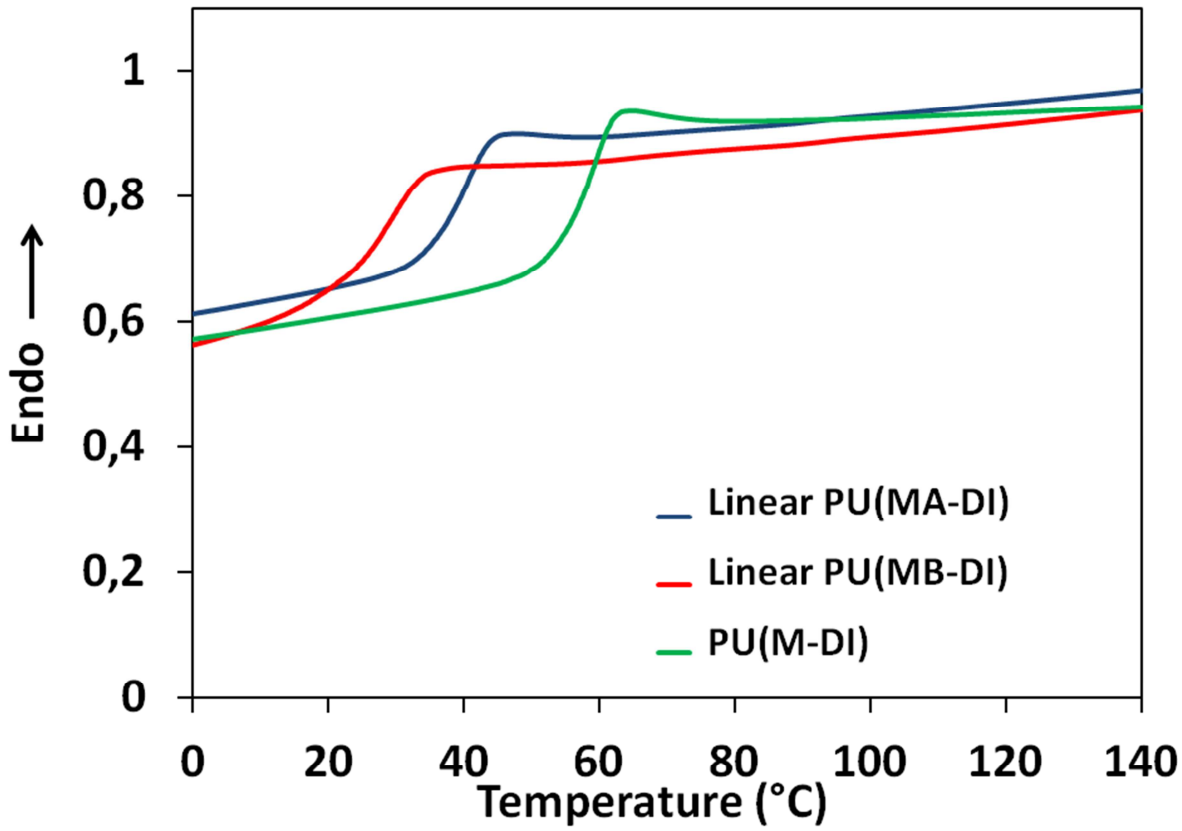

ACCEPTED MANUSCRIPT

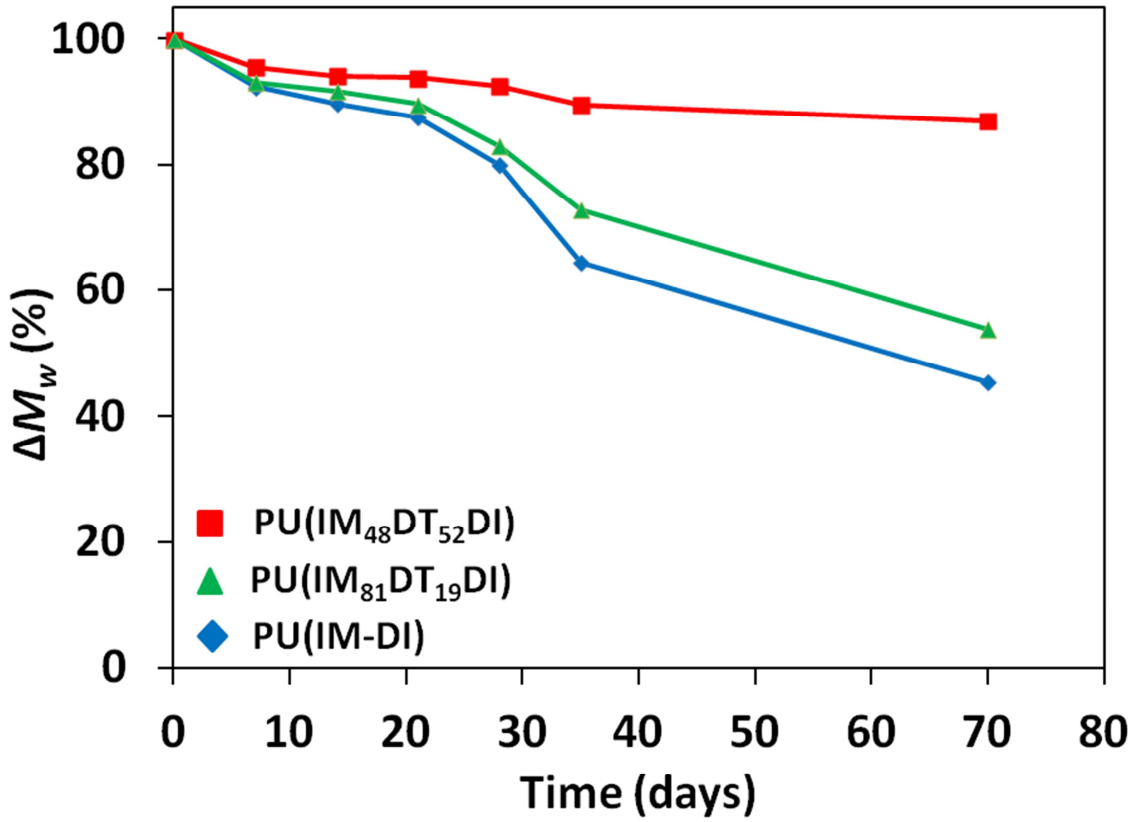

ACCEPTED MANUSCRIPT

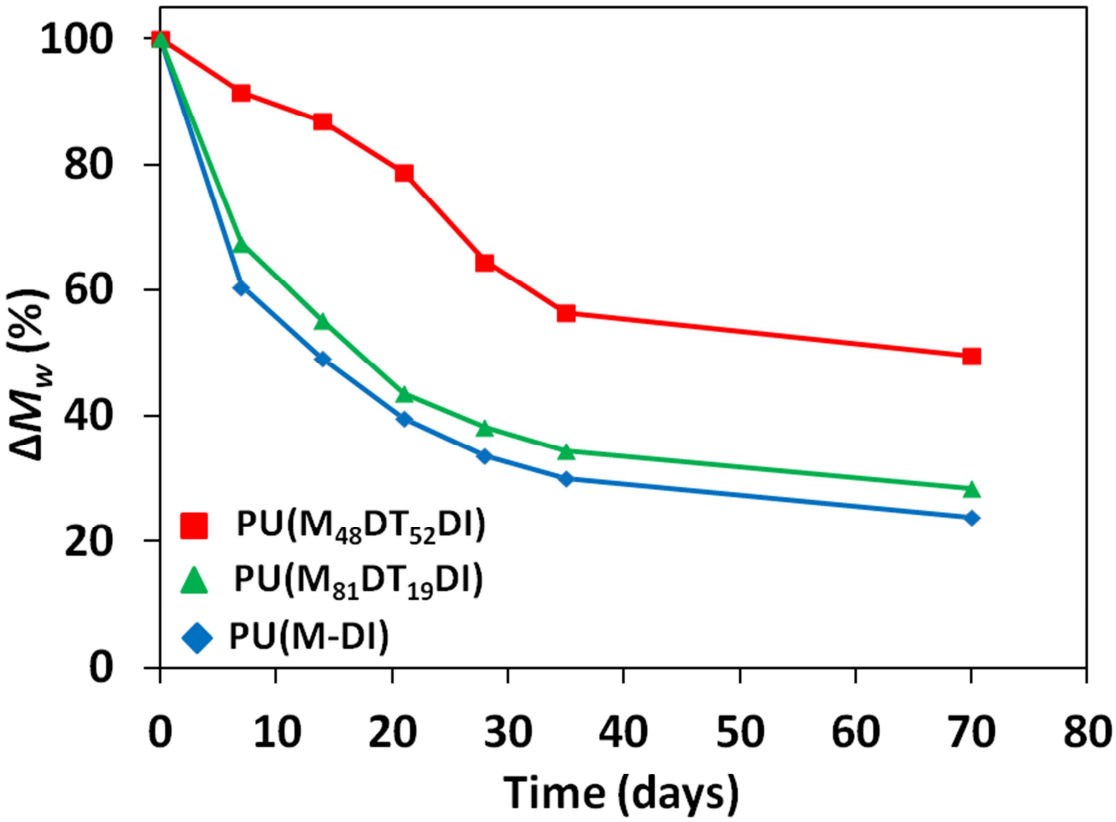

ACCEPTED MANUSCRIPT

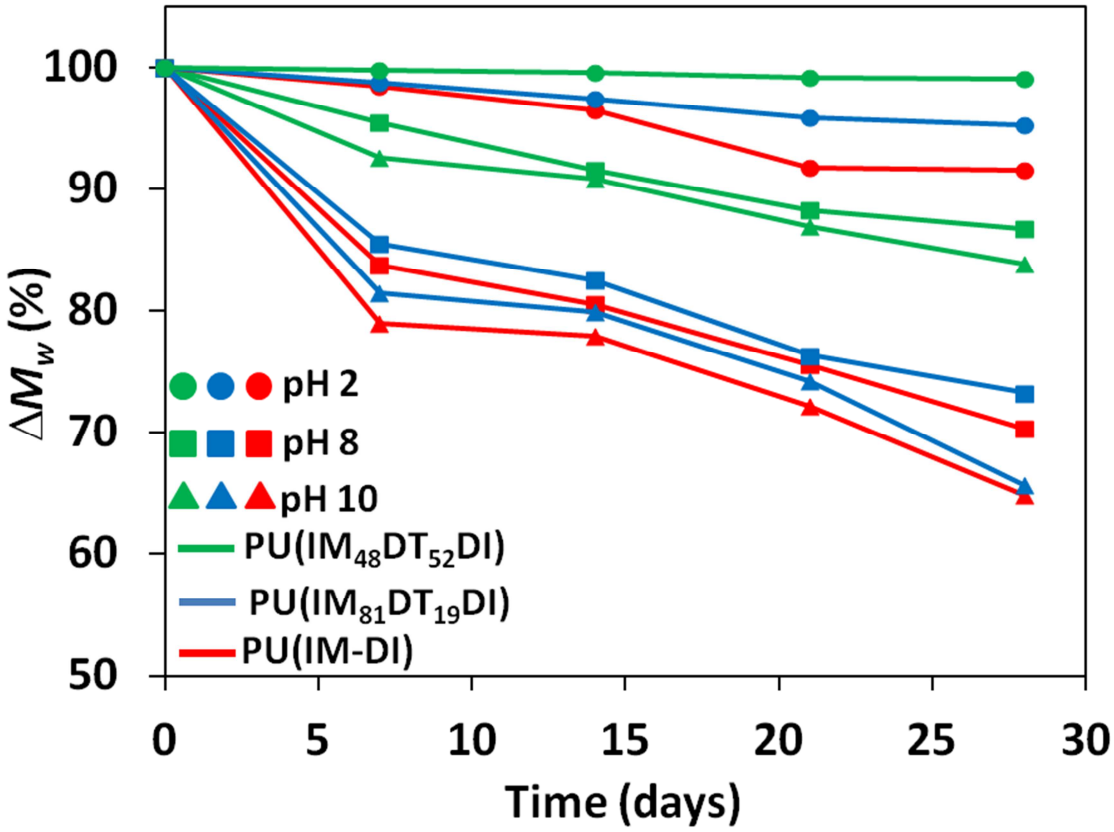

ACCEPTED MANUSCRIPT

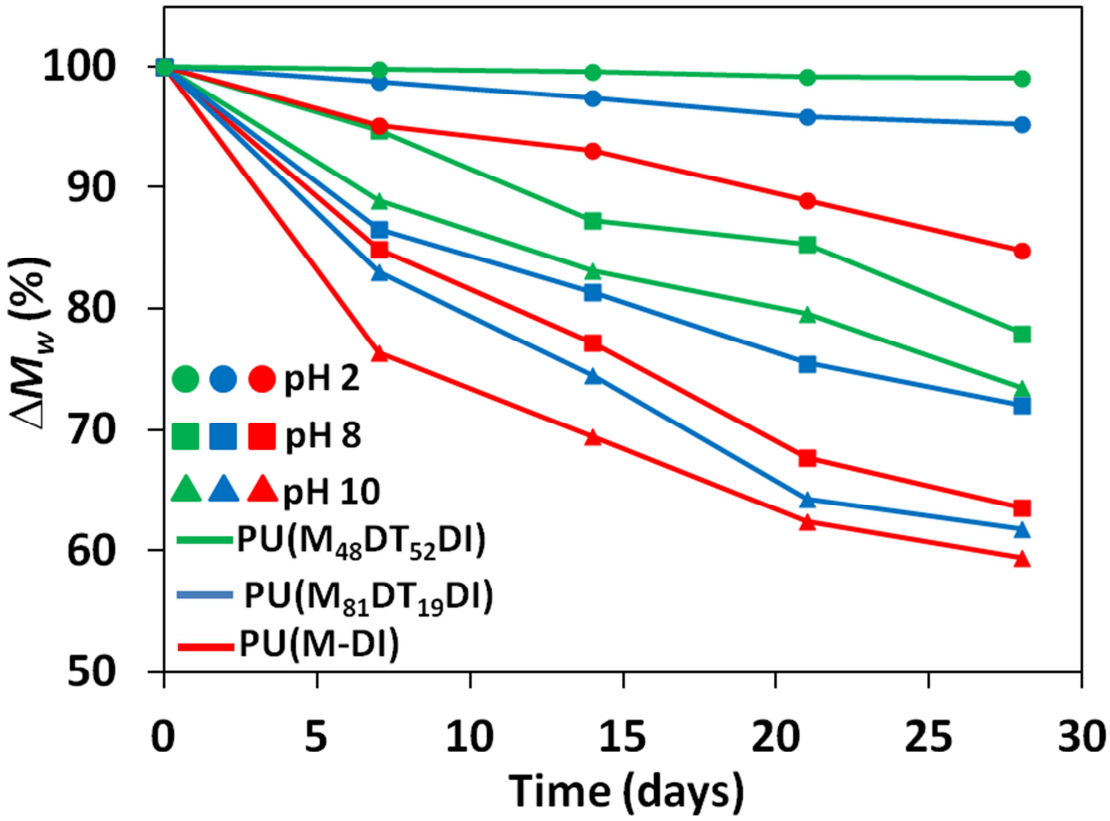

ACCEPTED MANUSCRIPT

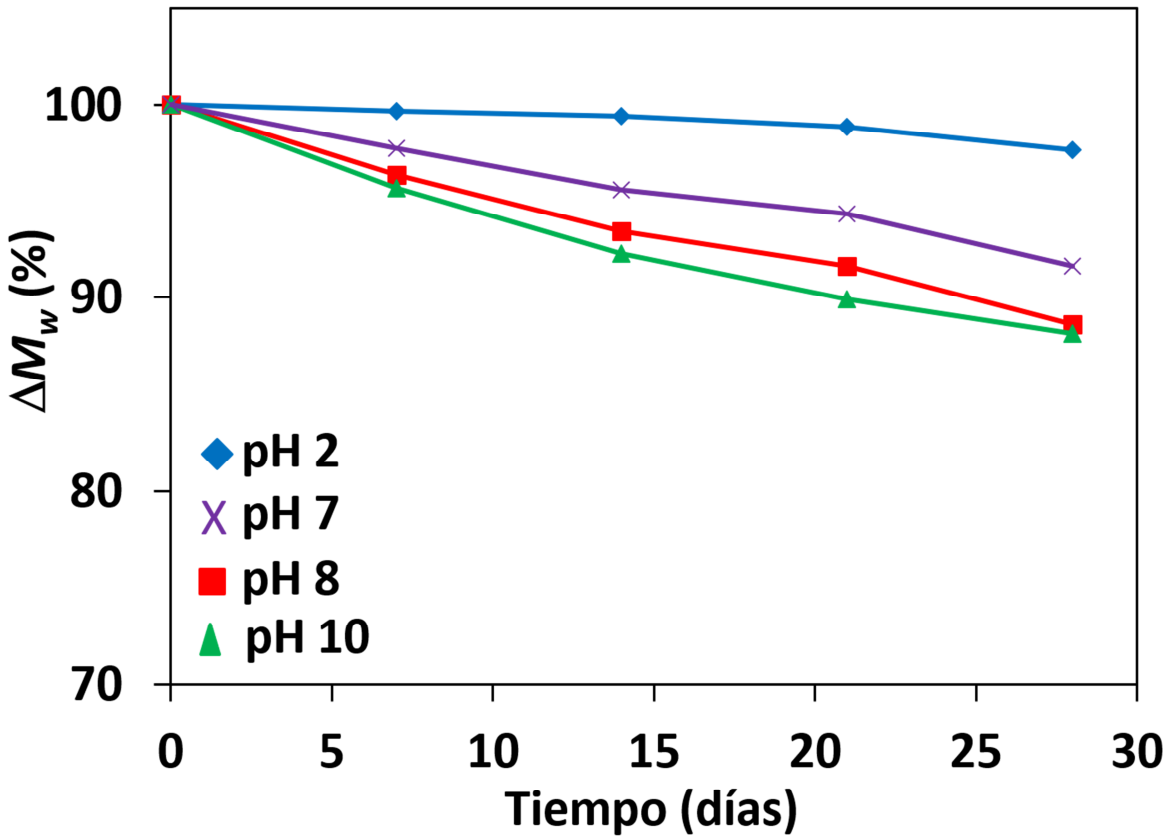

ACCEPTED MANUSCRIPT

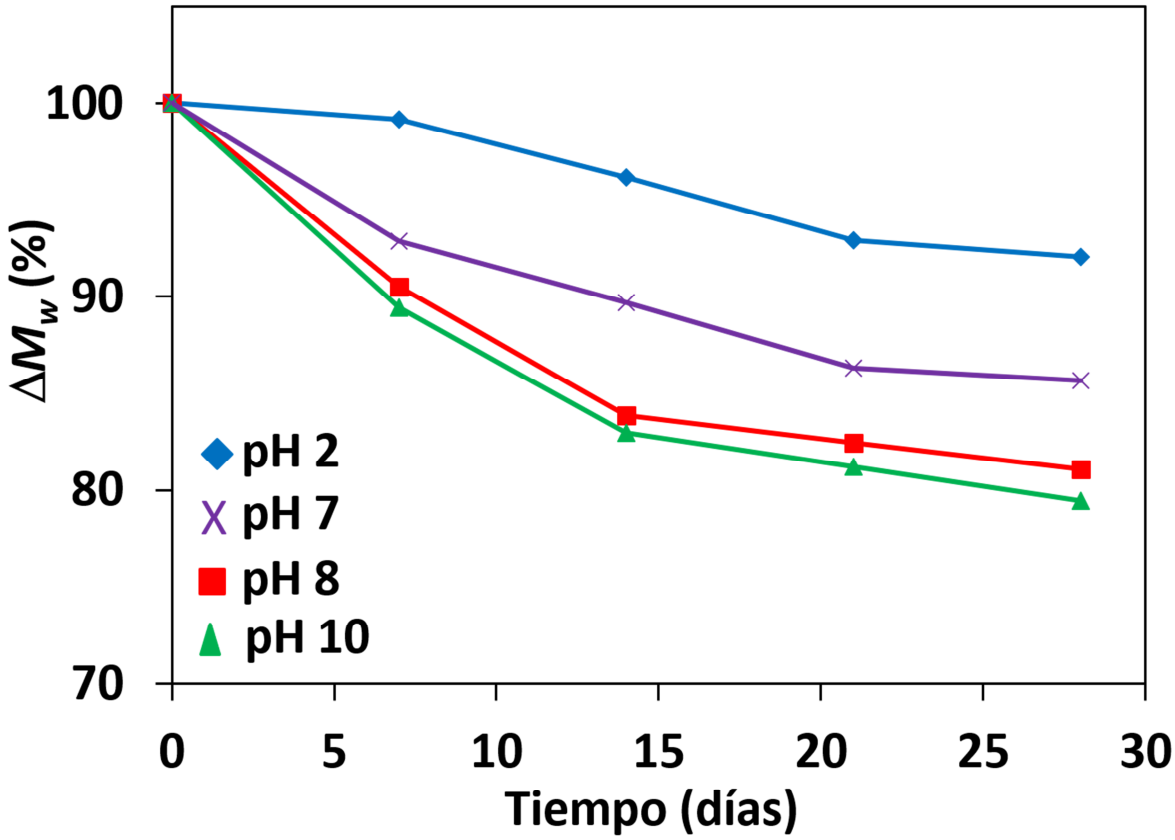

ACCEPTED MANUSCRIPT

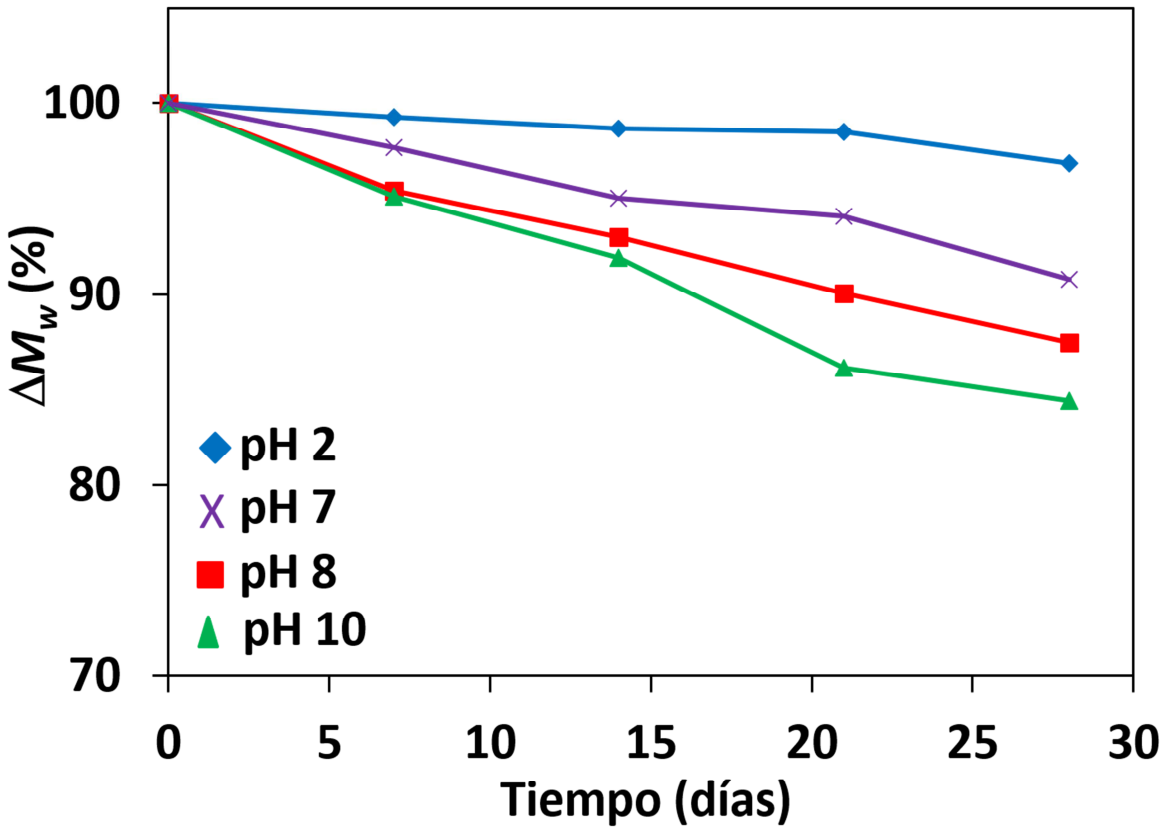

ACCEPTED MANUSCRIPT

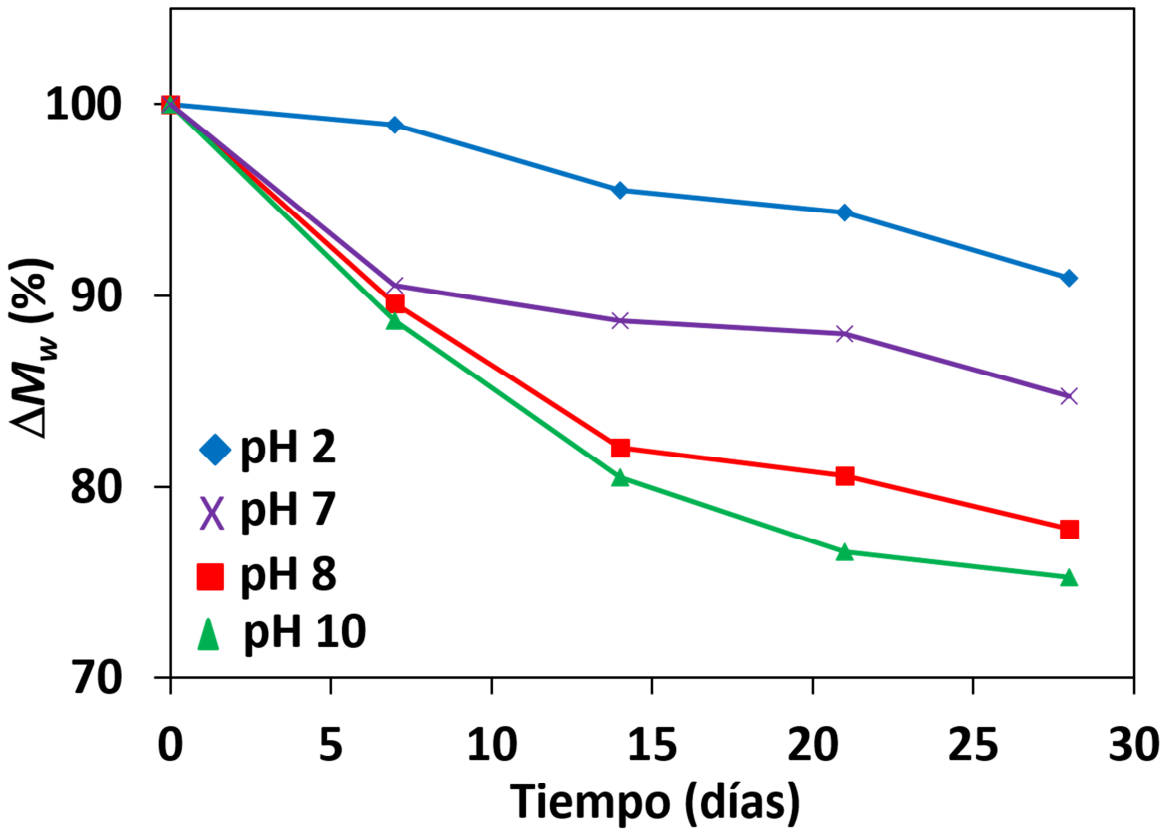

ACCEPTED MANUSCRIPT

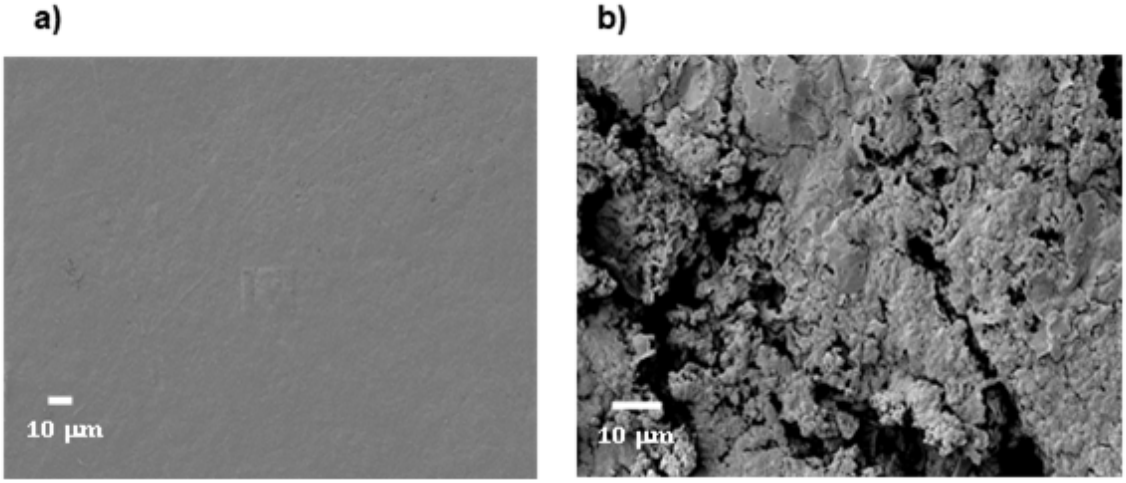

ACCEPTED MANUSCRIPT

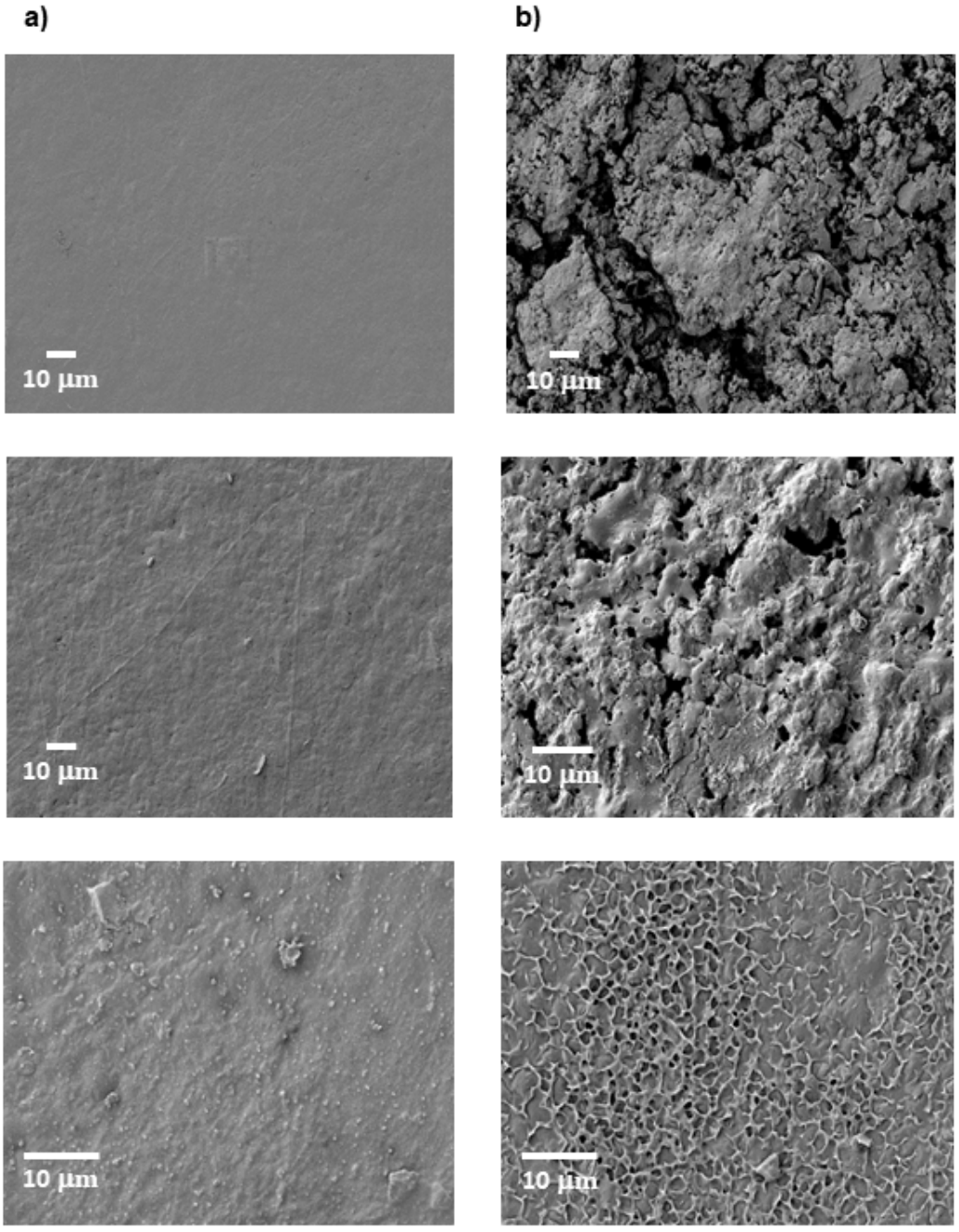
a)
b)
10 µm
10 µm
10 µm
10 µm
10 µm
10 µm

ACCEPTED MANUSCRIPT

Hydrolytic degradation of D-mannitol-based polyurethanes

Lucía Romero-Azogil,[†] Elena Benito,[†] Antxon Martínez de Ilarduya,[‡]
M. Gracia García-Martín[†]* and Juan A. Galbis[†]

*Corresponding author: graciagm@us.es

Highlights:

- Hydrolytic degradation of polyurethanes with proven sustained and site-specific drug release in the gastrointestinal tract
- Hydrophilic carbohydrate-based polyurethanes with enhanced degradation under physiological conditions
- Branching and linearity of D-mannitol-based polyurethanes determine the scope of hydrolytic degradation processes.

ACCEPTED MANUSCRIPT